Paper IV

Biochemical characterization of isocitrate dehydrogenase from *Methylococcus capsulatus* reveals a unique NAD^+-dependent homotetrameric enzyme

Runar Stokke[1], Dominique Madern[2], Anita-Elin Fedøy[1], Solveig Karlsen[3], Nils-Kåre Birkeland[1]and Ida Helene Steen[1*],

Department of Biology, University of Bergen, P.O. Box 7800, N-5020 Bergen, Norway[1]; Laboratoire de Biophysique Moleculaire, Institut de Biologie Structurale J.-P. Ebel CEA CNRS UJF, UMR-5075, 41 rue Jules Horowitz, 38027 Cedex 01, Grenoble, France[2] and The Norwegian Structural Biology Centre (NORSTRUCT), University of Tromsø, N-9037 Tromsø, Norway[3]

*Corresponding author: Ida Helene Steen Tel: +47 - 55 58 83 75; Fax +47 – 55589671

Email: Ida.Steen@bio.uib.no

Abstract

The gene encoding isocitrate dehydrogenase (IDH) of *Methylococcus capsulatus* (*Mc*IDH) was cloned and overexpressed in *Escherichia coli*. The purified enzyme was NAD^+-dependent with a thermal optimum for activity at 55-60 ºC and an apparent midpoint melting temperature (T_m) of 70.3 ºC. Analytical ultracentrifugation (AUC) revealed a homotetrameric state and *Mc*IDH thus represents the first homotetrameric NAD^+-dependent IDH characterized. Based on a structural alignment of *Mc*IDH and homotetrameric homoisocitrate dehydrogenase (HDH) from *Thermus thermophilus* (*Tt*HDH), we identified the clasp-like domain of *Mc*IDH as a likely site for tetramerization. *Mc*IDH showed moreover, higher sequence identity (48%) to *Tt*HDH than to previously characterized IDHs. Putative NAD^+-IDHs with high sequence identity (48-57%) to *Mc*IDH were however; identified in a variety of bacteria showing that NAD^+-dependent IDHs are indeed widespread within the domain Bacteria. As their primary structures are highly similar to HDH and isopropylmalate dehydrogenase (IPMDH) it is likely that they represent the present day mirrors of an ancient form of IDH.

Keywords: β-Decarboxylating dehydrogenase; *Methylococcus capsulatus*; Isocitrate dehydrogenase; Isopropylmalate dehydrogenase; Homoisocitrate dehydrogenase; Cofactor specificity; Tetrameric

Introduction

β-Decarboxylating dehydrogenases are a family of bifunctional enzymes that catalyze the Mg^{2+}- and $NAD(P)^{+}$- dependent dehydrogenation at C2 followed by their Mg^{2+}-dependent decarboxylation at C3 of (2R, 3S) 2- hydroxy acids producing 2-Keto acid, CO_2 and reduced coenzyme. Four orthologs have been identified so far: NAD^{+}-dependent isocitrate dehydrogenase (EC 1.1.1.41, NAD^{+}-IDH), $NADP^{+}$-dependent IDH (EC 1.1.1.42, $NADP^{+}$-IDH), NAD^{+}-dependent isopropylmalate dehydrogenase (EC 1.1.1.85, NAD^{+}-IPMDH), and homoisocitrate dehydrogenase (EC 1.1.1.115, HDH). Furthermore, tartrate dehydrogenase (TDH) has been suggested as a member of this enzyme family (Tipton and Beecher, 1994).

IDH and IPMDH have been characterized from a variety of organisms and they share a common protein fold that lacks the βαβαβ motif characteristic of the nucleotide binding Rossman fold (Hurley *et al.*, 1989a; Imada *et al.*, 1991). They are however, highly specific for their substrate, isocitrate and isopopropylmalate, respectively (Imada *et al.*, 1998; Miyazaki *et al.*, 1993; Zhang and Koshland, 1995). In contrast, HDHs have been characterized showing both duplicate and triplicate substrate specificity, a property probably found among primitive decarboxlating dehydrogenases (Miyazaki, 2005a, b).

A number of three-dimensional structures has been resolved for homodimeric β-decarboxylating dehydrogenase whereas only HDH from *Thermus thermophilus* (*Tt*HDH) has been resolved in a homo-tetrameric form (Ceccarelli *et al.*, 2002; Hurley *et al.*, 1989; Imada *et al.*, 1991; Karlström *et al.*, 2005; Miyazaki *et al.*, 2005; Singh *et al.*, 1999; Singh *et al.*, 2002; Wallon *et al.*, 1997; Xu *et al.*, 2004). In homodimeric IDH each subunit can be divided into three domains; a large α + β domain, a small α/β domain, and a clasp-like domain functioning as an interlock holding the two subunits together. The clasp domain varies substantially in primary sequence and differs in the three-dimensional structures and these differences have been suggested to serve as indicators for phylogentic and evolutionary analysis of IDH (Xu *et al.*, 2004). In HDH and IPMDH the clasp domain is substituted by an

arm-like protrusion and in HDH this arm-like protrusion is proven to be involved in tetramerization (Imada *et al.*, 1991; Miyazaki *et al.*, 2005).

Although IDH is a well-characterized enzyme, most IDHs investigated are $NADP^+$-IDHs. $NADP^+$-IDH is widely distributed throughout the three domains of life. With the exception of the homotetrameric IDH from *Thermotoga maritima* (*Tm*IDH) and a few monomeric IDHs, all characterized $NADP^+$-IDHs have been found to be homodimeric (Steen *et al.*, 2001). NAD^+-dependency is in contrast restricted to eukaryal hetero-oligomeric IDHs, a few homodimeric bacterial IDHs and one homodimeric archaeal IDH (Steen *et al.*, 2001). By characterization of IDH from *Methylococcus capsulatus* (*Mc*IDH), we have identified the first homotetrameric NAD^+-dependent IDH. *Mc*IDH showed high sequence identity to the homotetrameric *Tt*HDH and structural alignment of *Mc*IDH and *Tt*HDH revealed the clasp-like domain as a likely tetramerization-site in *Mc*IDH. A widespread occurrence of NAD^+-IDH similar to *Mc*IDH across the domain Bacteria was observed and the implications of these findings are discussed herein.

Materials and methods

Protein production

Putative *icd* gene (MCA3071) from *M. capsulatus* (Ward *et al.*, 2004) was amplified from genomic DNA by PCR using the following primers respectively; 5`-CACCATGCACAAGATCACCCTCAT-3` and 5`- AAGCTTCTACGCCTGACGCAC-3`. The PCR product was purified using the Stratagene PCR Purification Kit, and ligated into pET101/D-TOPO from Invitrogen. Recombinant *Mc*IDH was overexpressed in *Escherichia coli* strain BL21-CodonPlus(DE3)-RIL by growing transformed cells in LB broth containing ampicillin (100 μg ml^{-1}) at 37ºC to OD_{600} = 0.7-0.8 cell density and subsequent expression (3-4 h) after addition of 1.0 mM isopropyl-β-D-thio-galactopyranoside. Cells resuspended in 20 mM sodium phosphate buffer (pH 7.0) containing 10 mM $MgCl_2$ were disrupted using a

French pressure cell. After removal of cell debris by centrifugation (13000*g*, 30 min) the cell extract was subjected to heat treatment at 60°C for 20 min. Precipitated protein was removed by centrifugation (15000*g*, 30 min) and the heat treated extracts were applied to a Red Sepharose column (Millipore). Fractions containing IDH activity were eluted with a 0-2 M NaCl gradient over 2 hours, pooled and concentrated with a VivaScience spin coloumn.

The purity of the recombinant enzymes was confirmed by SDS-PAGE and protein concentration was measured by the method of Bradford (Bradford, 1976).

Enzyme assay

The enzyme reactions were measured photometrically at 45°C by monitoring the formation of NAD(P)H at 340 nm ($\varepsilon_{340} = 6.22 \cdot mM^{-1} \cdot cm^{-1}$) using a CARY UV spectrophotometer. The standard reaction of 1 ml contained 50 mM Tricine-KOH pH 8.0, 0.25 mM NAD^+, 1 mM isocitrate and 10 mM $MgCl_2$. One Unit of enzyme activity is the reduction of 1 µmol of $NAD(P)^+$ per minute. For determination of $K_{m\ NAD^+}$ and $V_{max\ NAD^+}$, the isocitrate concentration was kept fixed at 1 mM while varying the cofactor concentration. For determination of $K_{m\ isocitrate}$ and $V_{max\ isocitrate}$ values, the cofactor concentration was kept fixed at 0.25 mM whilst varying the isocitrate concentration. The data were analyzed by the direct linear plot of Eisenthal and Cornish-Bowden (Eisenthal and Cornish-Bowden, 1974) using the Enzpack 3 software package (Biosoft, Cambridge, UK).

Oligomeric state

Analytical ultracentrifugation (AUC) experiments were performed using a Beckman XLI analytical ultracentrifuge equipped with a UV scanning system, using a 4-hole AN-60 Ti rotor with double-channel centrepieces of 1.20 cm path length. Two hundred absorbance profiles were recorded at 20°C and 42,000 rpm, analysed by the Sedfit program (Schuck, 2000) The

calculation of the corrected sedimentation coefficient at 20°C in water ($s_{20,w}$) was performed as described previously (Steen *et al.*, 2001) .

Size exclusion chromatography was done using a HiLoad 16/60 Superdex column (Amersham Biosciences, 1.6 × 60 cm) equilibrated with 50 mM potassium phosphate buffer (pH 7.5), containing 0.1 M NaCl. Homodimeric and homotetrameric *Tm*IDH (90.8 and 181.6 kDa, respectively) as well as homodimeric IDH from *Aeropyrum pernix* (*Ap*IDH, 95.8 kDa) (Steen *et al.*, 2001) were used as standards.

Thermal activity and stability

Determination of the thermal optimum of activity was performed at different temperatures ranging from 30 – 70°C according to standard reaction described above (pH of reaction buffer was adjusted to 8.0 at the given temperatures).

Differential scanning calorimetry (DSC) was carried out with a MicroCal calorimeter. The protein sample was dialyzed against the reference buffer used in the experiment [50 mM potassium phosphate buffer (pH 7.5) and 0.1 M NaCl]. A protein concentration of 1.5 mg ml^{-1} was used and the calorimetric scans were carried out between 20 and 90°C with a scan rate of 60ºC h^{-1}. The thermogram was baseline subtracted and normalized for protein concentration.

Primary sequence analysis

Genes encoding proteins related to *Mc*IDH were identified using the BLAST algorithm. Identified putative IDHs were aligned to the structural alignment presented in Fig. 1 using Clustal X (Thompson *et al.*, 1997) and then edited using GeneDoc (http://www.psc.edu/biomed/genedoc/ebinet.htm). The alignment is available from the authors on request. Pair wise sequence comparisons were done using the BLAST 2 algorithm at http://www.ncbi.nlm.nih.gov/blast/bl2seq/wblast2.cgi**.**

Results and discussion

Biochemical characterization of McIDH

Characterization of *Mc*IDH revealed a thermostable homotetrameric NAD^+-dependent enzyme. When the cofactor specificity of *Mc*IDH was determined at 45°C in 50 mM Tricine-KOH (pH 8.0) including 10 mM Mg^{2+} and 1 mM D,L-isocitrate using NAD^+ and $NADP^+$, no activity was detected for $NADP^+$ (when using concentration up to 2 mM). As predicted from the conservation of the Asp^{268} and Ile^{269} residues corresponding to Asp^{278} and Ile^{279} in *T. thermophilius* (*Tt*IPMDH; Fig. 1), *Mc*IDH was NAD^+-dependent. The K_m determined for NAD^+ was 122.0 μM. *Mc*IDH had a K_m of 51.7 μM for D,L-isocitrate and the substrate specificity determinants in *E. coli* IDH (*Ec*IDH), Ser^{113} and Asn^{115} were conserved in *Mc*IDH (Fig. 1).

*Mc*IDH had a thermal optimum for activity at 55 – 60ºC (not shown). An apparent midpoint melting temperature (T_m) of 70.3˚C was found when DSC was performed in potassium phosphate buffer (pH 7.5) containing 0.1 M NaCl (Fig. 2). The thermal unfolding was irreversible and the asymmetry of the curve a consequence of aggregation. Hence, only an apparent T_m could be determined. The thermophilic character of the enzyme was as expected from the moderately thermophilic nature of the source organism. However, the T_m of *Mc*IDH was almost 20ºC higher than the previously determined T_m of 52.6ºC for mesostable *Ec*IDH whereas the growth optimum of *M. capsulatus* is only 8ºC higher than that of *E. coli*. Hence, comparing the growth optimum of the two source organisms, the T_m of *Mc*IDH is relatively higher than that of *Ec*IDH. The T_m determined for *Mc*IDH was as expected lower than the T_m -values of 109.9, 103.7, 98.3 and 98.5ºC as previously determined for hyperthermostable IDH from *A. pernix*, *Pyrococcus furiosus, T. maritima* and *Archaeoglobus fulgidus*, respectively (Steen *et al.*, 2001).

A subunit molecular mass of 36340.3 Dalton was calculated from the primary structure of *Mc*IDH using the ProtParam tool at the ExPACY server

(http://au.expasy.org/tools/protparam.html). This values is similar to the subunit molecular mass of IPMDH and HDH and eukaryal hetero-oligomeric IDHs and lower that the value around 42 KDa typical found for homodimeric $NADP^+$-IDHs.

In order to estimate the oligomeric state of *Mc*IDH, the protein was analysed using molecular size exclusion chromatography on a HiLoad 16/60 Superdex column. *Mc*IDH eluted before the homodimeric *Ap*IDH with an elution volume suggesting a species of higher molecular weight. A sedimentation velocity analysis on *Mc*IDH was done to analyse its association state with a greater accuracy. A single run of analytical centrifugation was recorded using a protein concentration of 0.1 mg ml^{-1}. The sedimentation coefficient distribution (Fig. 3), shows a major peak with a $s_{20,\,w}$ of 7.4 S. This value is close to the theoritical s value of 8.0 S expected for globular tetramer. A minor peak with a s value of 3.7 S is also observable. The AUC data were analysed using the non-interacting species option of Sedfit with the minor peak considered as a heterologous species. The calculated molecular mass of *Mc*IDH was 142 kDa, a value in agreement with the expected value of 145 kDa for a tetramer.

Previously, we have described IDH as a family of enzymes that include five different oligomeric forms as follows: hetero-oligomeric NAD^+-IDHs, homodimeric NAD^+-IDHs, monomeric $NADP^+$-IDHs, homodimeric $NADP^+$-IDHs and homotetrameric IDHs $NADP^+$-IDHs (Steen *et al.*, 2001). All IPMDHs are NAD^+-dependent and most of them are homodimeric although a homotetrameric oligomeric state has been identified for IPMDH from *Sulfolobus* sp. Strain 7 (Suzuki *et al.*, 1997). HDH from *T. thermophilus* and *Deinococcus radiodurans* are both homotetrameic (Miyazaki *et al.*, 2005; Miyazaki, 2005b). The homoteramеric state observed for the NAD^+-dependent *Mc*IDH represents a new oligomeric state of NAD^+-IDH. By implication, homotetrameric NAD^+-dependent enzymes are present in three of the orthologs forming the family of β-decarboxylating dehydrogenases.

Prediction of the tetramerization site in *Mc*IDH

A number of three-dimensional structures have been resolved for homodimeric β-decarboxylating dehydrogenase, however, the only structure resolved in a homotetrameric form is *Tt*HDH (Miyazaki *et al.*, 2005). In *Tt*HDH the arm-like protrusion of the clasp-domain is involved in tetramer formation via hydrophobic interactions (Miyazaki *et al.*, 2005). Val^{135} contributes to a hydrophobic environment with Tyr^{125} and Val^{141} from another subunit of the same dimer and Tyr^{132} and Leu^{133} from the second dimer. A Val^{135}Met mutation was shown to cause a tetramer-to-dimer transition of the quaternary structure (Miyazaki *et al.*, 2005). In order to identify the tetramerization site in *Mc*IDH, a model of the subunit structure was constructed using *Tt*HDH as template (Fig. 4). In the clasp-region of the *Mc*IDH model structure, hydrophobic residues were observed in the same positions as in *Tt*HDH (Fig. 4). Although not perfectly aligned due to a 6 residues insertion in the clasp-region of *Mc*IDH (Fig. 1), it is very likely that Val^{132}, Tyr^{123} and Val^{144} (Val^{135}, Tyr^{125} and Val^{141} in *Tt*HDH) contributes to a hydrophobic environment with Phe^{129} and Ile^{130} (corresponding to Tyr^{132} and Leu^{133} in *Tt*HDH) (Fig. 4). Thus, it is believed that tetramer formation in *Mc*IDH is achieved through hydrophobic interactions between the two clasp-like domains.

Site-directed mutagenesis altering the homo-tetrameric *Tt*HDH to a homodimeric enzyme resulted in a markedly decreased thermal inactivation temperature indicating that tetramer formation was involved in the extreme thermostability of this enzyme (Miyazaki *et al.*, 2005). A higher oligomeric state has also been found in other (hyper)thermophilic enzymes (Vieille and Zeikus, 2001). The homotetrameric state of *Mc*IDH may thus partly explain the relatively higher T_m than that observed for *Ec*IDH.

Primary sequence analysis

Among previously characterized IDHs, *Mc*IDH was most similar to eukaryal allosterically regulated NAD^+-dependent IDHs with a sequence identity of 42% when compared with the catalytic subunit of yeast (NAD^+-IDH 2). Only 35% sequence identity was found when *Mc*IDH was compared with *Ec*IDH. Interestingly, *Mc*IDH showed higher sequence identity to *Tt*HDH (48%) than to previously characterized IDHs and the sequence identity was also high toward *Tt*IPMDH (35%). *Mc*IDH did however; show highest sequence identity (48 – 57%) to the putative IDHs listed in Table 1. Interestingly, most of the *Mc*IDH-like enzymes included in Table 1 are comprised of between 332 - 340 amino acid residues. This is the same number of amino acids as in IPMDH and HDH as well as for eukaryal NAD^+-IDHs when the signal sequence is removed from these IDHs. Although IDH and IPMDH are defined as enzymes with the same overall structure (Hurley *et al.*, 1989a; Imada *et al.*, 1991), there are a few unique structural characteristics for the two enzymes. With the exception of the above mentioned eukaryal NAD^+-IDHs, IPMDHs have in general fewer amino acid residues than IDHs; *Tt*IPMDH has 345 amino acid residues compared with 416 in *Ec*IDH i. e. 71 residues less than *Ec*IDH. *Tt*HDH has 334 amino acid residues. The main difference responsible for the shorter sequence of *Tt*IPMDH compared with *Ec*IDH is that the clasp region consists of only one four-stranded anti-parallel β-sheet instead of two and that the clasp of *Tt*IPMDH lacks the helix corresponding to *Ec*IDH helix e (Fig. 1). Furthermore, the central β-sheet in *Tt*IPMDH s is comprised of 10 strands instead of 12 strands as in *Ec*IDH, and *Tt*IPMDH lacks the strands corresponding to *Ec*IDH strand K and L (Fig. 1). Recently, the crystal structure of *Tt*HDH was resolved and the subunit structure was highly similar to *Tt*IPMDH with a similar clasp region and central 10 stranded β-sheet (Miyazaki *et al.*, 2005). The structure-based alignment presented in Fig. 1 shows that *Mc*IDH has the same deletions in the primary structure as *Tt*IPMDH and *Tt*HDH when compared to *Ec*IDH. The same deletions also account for the reduced number of amino acid residues in the *Mc*IDH -like enzymes in Table 1, except for IDHs from the cyanobacteria, from cloroflexi and $NADP^+$-IDH from

Blastopirellula marina which seem to have a similar clasp as *Ec*IDH (sequences not shown). By implication the overall subunit structure of these IDHs is more similar to both *Tt*IPMDH and *Tt*HDH than to the overall subunit structure of *Ec*IDH. It should be noted that all IDHs represented in Table 1 carry residues corresponding to Ser^{113} and Asn^{115} in *Ec*IDH (Fig. 1) and hence carry the residues involved in isocitrate specificity. Furthermore, based on signature sequences for cofactor specificity the IDHs presented in Table 1 include both NAD^+- and $NADP^+$-dependent IDHs. It has been suggested that NAD^+-specificity emerged before $NADP^+$-specificity among IDH (Dean and Golding, 1997). Despite this, the most widespread form of IDHs have until now been the homodimeric $NADP^+$-dependent IDHs. The data presented in this paper show that the NAD^+-dependent form, similar to *Mc*IDH, is indeed widespread among the bacteria. Their high similarity to HDH and IPMDH indicate that they represent an ancient form of IDH and the presence of $NADP^+$-signatures among these enzymes indicates that $NADP^+$-specificity first evolved among these IDHs.

Acknowledgements

This work was supported by the Norwegian Research Council (Project no. 153774/420). The Norwegian Structural Biology Centre (NORSTRUCT) is supported by the national Functional Genomics Programme (FUGE) of the Research Council of Norway. We are grateful to Dr. Aurora Martinez, Department of Biomedicine, University of Bergen, for access to her laboratory facilities and expertise in use of differential scanning calorimetry. The excellent laboratory skills of Lisbeth Glærum and Marit Steine Madsen are also much appreciated.

References

Bradford, M.M. (1976) A rapid and sensitive method for the quantification of microgram quantities of protein utilizing the principle of protein-dye binding. *Anal. Biochem.* **7**: 248-254.

Ceccarelli, C., Grodsky, N.B., Ariyaratne, N., Colman, R.F., and Bahnson, B.J. (2002) Crystal structure of porcine mitochondrial $NADP^{(+)}$-dependent isocitrate dehydrogenase complexed with Mn^{2+} and isocitrate - Insights into the enzyme mechanism. *J. Biol. Chem.* **277**: 43454-43462.

Dean, A.M., and Golding, G.B. (1997) Protein engineering reveals ancient adaptive replacements in isocitrate dehydrogenase. *Proc. Natl. Acad. Sci. USA* **94**: 3104-3109.

Eisenthal, R., and Cornish-Bowden, A. (1974) Direct linear plot - new graphical procedure for estimating enzyme kinetic-parameters. *Biochem. J.* **139**: 715-720.

Gouet, P., Courcelle, E., Stuart, D.I., and Metoz, F. (1999) ESPript: analysis of multiple sequence alignments in PostScript. *Bioinformatics* **15**: 305-308.

Hurley, J.H., Thorsness, P.E., Ramalingam, V., Helmers, N.H., Koshland, D.E.J., and Stroud, R.M. (1989) Structure of a bacterial enzyme regulated by phosphorylation, isocitrate dehydrogenase. *Proc. Natl. Acad. Sci. USA* **86**: 8635-8639.

Imada, K., Sato, M., Tanaka, N., Katsube, Y., Matsuura, Y., and Oshima, T. (1991) 3-Dimensional structure of a highly thermostable enzyme, 3-isopropylmalate dehydrogenase of *Thermus thermophilus* at 2.2 Å resolution. *J. Mol. Biol.* **222**: 725-738.

Imada, K., Inagaki, K., Matsunami, H., Kawaguchi, H., Tanaka, H., Tanaka, N., and Namba, K. (1998) Structure of 3-isopropylmalate dehydrogenase in complex with 3-isopropylmalate at 2.0 angstrom resolution: the role of Glu88 in the unique substrate-recognition mechanism. *Structure with Folding & Design* **6**: 971-982.

Karlström, M., Stokke, R., Steen, I.H., Birkeland, N.K., and Ladenstein, R. (2005) Isocitrate dehydrogenase from the hyperthermophile *Aeropyrum pernix*: X-ray structure analysis of a ternary enzyme-substrate complex and thermal stability. *J. Mol. Biol.* **345**: 559-577.

Miyazaki, J., Asada, K., Fushinobu, S., Kuzuyama, T., and Nishiyama, M. (2005) Crystal structure of tetrameric homoisocitrate dehydrogenase from an extreme thermophile, *Thermus thermophilus*: Involvement of hydrophobic dimer-dimer interaction in extremely high thermotolerance. *J. Bact.* **187**: 6779-6788.

Miyazaki, K., Kakinuma, K., Terasawa, H., and Oshima, T. (1993) Kinetic-analysis on the substrate-specificity of 3-isopropylmalate dehydrogenase. *Febs Letters* **332**: 35-36.

Miyazaki, K. (2005a) Bifunctional isocitrate-homoisocitrate dehydrogenase: A missing link in the evolution of beta-decarboxylating dehydrogenase. *Biochem. Biophys. Res. Com.* **331**: 341-346.

Miyazaki, K. (2005b) Identification of a novel trifunctional homoisocitrate dehydrogenase and modulation of the broad substrate specificity through site-directed mutagenesis. *Biochem. Biophys. Res. Com.* **336**: 596-602.

Schuck, P. (2000) Size-distribution analysis of macromolecules by sedimentation velocity ultracentrifugation and Lamm equation modeling. *Biophys. J.l* **78**: 1606-1619.

Singh, S.K., Miller, S.P., Matsuno, K., Sonenshein, A.L., LaPorte, D.C., and Banaszak, L.J. (1999) Crystal structure of isocitrate dehydrogenase from *B. subtilis*. *Faseb Journal* **13**: A1560-A1560.

Singh, S.K., Miller, S.P., Dean, A., Banaszak, L.J., and LaPorte, D.C. (2002) *Bacillus subtilis* isocitrate dehydrogenase - A substrate analogue for *Escherichia coli* isocitrate dehydrogenase kinase/phosphatase. *J. Biol.Chem.y* **277**: 7567-7573.

Steen, I.H., Madern, D., Karlström, M., Lien, T., Ladenstein, R., and Birkeland, N.K. (2001) Comparison of isocitrate dehydrogenase from three hyperthermophiles reveals differences in thermostability, cofactor specificity, oligomeric state, and phylogenetic affiliation. *J. Biol. Chem.***276**: 43924-43931.

Suzuki, T., Inoki, Y., Yamagishi, A., Iwasaki, T., Wakagi, T., and Oshima, T. (1997) Molecular and phylogenetic characterization of isopropylmalate dehydrogenase of a thermoacidophilic archaeon, *Sulfolobus* sp strain 7. *J. Bact.* **179**: 1174-1179.

Thompson, J.D., Gibson, T.J., Plewniak, F., Jeanmougin, F., and Higgins, D.G. (1997) The CLUSTAL_X windows interface: flexible strategies for multiple sequence alignment aided by quality analysis tools. *Nucl. Acids Res.***25**: 4876-4882.

Tipton, P.A., and Beecher, B.S. (1994) Tartrate dehydrogenase, a new member of the family of metal-dependent decarboxylating R-hydroxyacid dehydrogenases. *Arch. Biochem. Biophys.***313**: 15-21.

Vieille, C., and Zeikus, G.J. (2001) Hyperthermophilic enzymes: sources, uses, and molecular mechanisms for thermostability. *Microbiol. Mol. Biol. Rev.* **65**: 1-43.

Wallon, G., Kryger, G., Lovett, S.T., Oshima, T., Ringe, D., and Petsko, G.A. (1997) Crystal structures of *Escherichia coli* and *Salmonella typhimurium* 3-isopropylmalate dehydrogenase and comparison with their thermophilic counterpart from *Thermus thermophilus*. *J.Mol.Biol.* **266**: 1016-1031.

Ward, N., Larsen, O., Sakwa, J., Bruseth, L., Khouri, H., Durkin, A.S., Dimitrov, G., Jiang, L.X., Scanlan, D., Kang, K.H., Lewis, M., Nelson, K.E., Methe, B., Wu, M., Heidelberg, J.F., Paulsen, I.T., Fouts, D., Ravel, J., Tettelin, H., Ren, Q.H., Read, T., DeBoy, R.T., Seshadri, R., Salzberg, S.L., Jensen, H.B., Birkeland, N.K., Nelson, W.C., Dodson, R.J., Grindhaug, S.H., Holt, I., Eidhammer, I., Jonasen, I., Vanaken, S., Utterback, T., Feldblyum, T.V., Fraser, C.M., Lillehaug, J.R., and Eisen, J.A. (2004) Genomic insights into methanotrophy: The complete genome sequence of *Methylococcus capsulatus* (Bath). *Plos Biology* **2**: 1616-1628.

Xu, X., Zhao, J.Y., Xu, Z., Peng, B.Z., Huang, Q.H., Arnold, E., and Ding, J.P. (2004) Structures of human cytosolic NADP-dependent isocitrate dehydrogenase reveal a novel self-regulatory mechanism of activity. *J.Biol. Chem.* **279**: 33946-33957.

Zhang, T., and Koshland, D.E. (1995) Modeling substrate binding in *Thermus thermophilus* isopropylmalate dehydrogenase. *Protein Science* **4**: 84-92.

TABLES

Table 1. Putative ICDHs with 48-57 % sequence identity to *Mc*-ICDH.

Species name	Class	Accession No.	Assignment	# Amino acid residues	Sequence identity to *Mc*-ICDH (%)
Rubrobacter xylanophilus	Actinobacteria*	**ZP_00600210**	NADP-ICDH	390	50
Gluconobacter oxydans	Alphaproteobacteria	**AAW61088**	NAD-ICDH	340	57
Rhodoferax ferrireducens	Betaproteobacteria	**ABD70128**	NAD-ICDH	345	52
Rhodoferax ferrireducens	Betaproteobacteria	**ABD70097**	NAD-ICDH	344	52
Dehalococcoides ethenogenes	Chloroflexi*	**AAW40236**	NADP-ICDH	359	50
Thermosynechococcus elongatus	Cyanobacteria*	**BAC07855**	NADP-ICDH	358	51
Moorella thermoacetica	Clostridia	**ABC19308**	NADP-ICDH	336	54
Clostridium acetobutylicum	Clostridia	**AAK78948**	NAD-ICDH	334	55
Caldicellulosiruptor saccharolyticus	Clostridia	**ZP_00886702**	NADP-ICDH	335	55
Carboxydothermus hydrogenoformans	Clostridia	**ABB13677**	NADP-ICDH	332	55
Halothermothrix orenii	Clostridia	**ZP_01188130**	NAD-ICDH	331	55
Cyanobacteria bacterium	Cyanobacteria*	**YP_477900**	NADP-ICDH	356	52
Bdellovibrio bacteriovorus	Deltaproteobacteria	**CAE79161**	NAD-ICDH	333	50
Alteromonas macleodii	Gammaproteobacteria	**ZP_01109532**	NAD-ICDH	335	52
Colwellia psychrerythraea	Gammaproteobacteria	**AAZ24724**	NAD-ICDH	335	52
Pseudoalteromonas haloplanktis	Gammaproteobacteria	**CAI89502**	NAD-ICDH	335	53
Pseudoalteromonas atlantica	Gammaproteobacteria	**ZP_00776245**	NAD-ICDH	335	53
Alkalilimnicola ehrlichei	Gammaproteobacteria	**ZP_00866330**	NAD-ICDH	335	53
Shewanella denitrificans	Gammaproteobacteria	**EAN71324**	NAD-ICDH	336	54
Shewanella frigidimarina	Gammaproteobacteria	**ZP_00638757**	NAD-ICDH	336	54
Shewanella amazonensis	Gammaproteobacteria	**ZP_00585518**	NAD-ICDH	336	54
Idiomarina loihiensis	Gammaproteobacteria	**AAV81701**	NAD-ICDH	334	54
Xanthomonas axonopodis	Gammaproteobacteria	**AAM35929**	NAD-ICDH	335	54
Shewanella oneidensis	Gammaproteobacteria	**NP_717154**	NAD-ICDH	335	55
Shewanella baltica	Gammaproteobacteria	**ZP_00580588**	NAD-ICDH	335	55
Pseudoalteromonas tunicata	Gammaproteobacteria	**ZP_01132005**	NAD-ICDH	335	55
Xanthomonas campestris	Gammaproteobacteria	**AAM40277**	NAD-ICDH	335	55
Xylella fastidiosa	Gammaproteobacteria	**ZP_00681714**	NAD-ICDH	335	56
Chromohalobacter salexigens	Gammaproteobacteria	**ZP_00473372**	NAD-ICDH	338	56
Idiomarina baltica	Gammaproteobacteria	**ZP_01043074**	NAD-ICDH	334	57
Gloeobacter violaceus	Cyanobacteria*	**BAC91029**	NADP-ICDH	359	51
Blastopirellula marina	Planctomycetes*	**ZP_01089525**	NADP-ICDH	366	48
Blastopirellula marina	Planctomycetes*	**ZP_01093589**	NAD-ICDH	338	51
Salinibacter ruber	Bacteroidetes*	**YP_445796**	NAD-ICDH	340	56

* = Phylum

LEGENDS TO FIGURES

Fig. 1.

Structure-based sequence alignment of *Mc*IDH (Accession No. AAU90861) with *Ec*IDH (Accession No. P08200), *Tt*IPMDH (Accession No. AAA16706) and *Tt*HDH (Accession No. AAS81354). Identical and similar residues are boxed. Residues involved in binding and substrate discrimination (Ser^{113} and Asn^{115}) in *Ec*IDH are marked with a square. Asp^{278} and Ile^{279} involved in NAD^+ specificity in *Tt*IPMDH and Lys^{344} and Tyr^{345} involved in $NADP^+$ specificity in *Ec*IDH are marked with an asteriks. The secondary structure of *Ec*IDH and *Tt*IPMDH are placed above and under the alignment, respectively. The nomenclature used for naming the secondary structure elements is from (Hurley *et al.*, 1989) and the figure was made with ESPript 2.2 (Gouet *et al.*, 1999).

Fig. 2. Thermal unfolding of *Mc*IDH as by differential scanning calorimetry.

Fig. 3. Sedimentation velocity analysis of *Mc*IDH at 20°C. The data recorded at 0.1 mg ml^{-1}, in 50 mM NaCl buffered with 50 mM Tris-HCl (pH 8) were fitted using the sedfit software (Schuck, 2000).

Fig. 4. (A) Structure of *Tt*HDH (1X0L.pdb) subunit A. Residues involved in tetramer formation are in blue. (B) Model structure of *Mc*IDH (constructed in SwissModel). Conserved amino acids in tetramer formation compared to *Tt*HDH are in red. (C) Structure of *Tt*IPMDH (1IPD.pdb) subunit A. (D) Structure of *Ec*IDH (1SJS.pdb) subunit A. The different clasp domains are in orange.

FIGURES

Fig.1

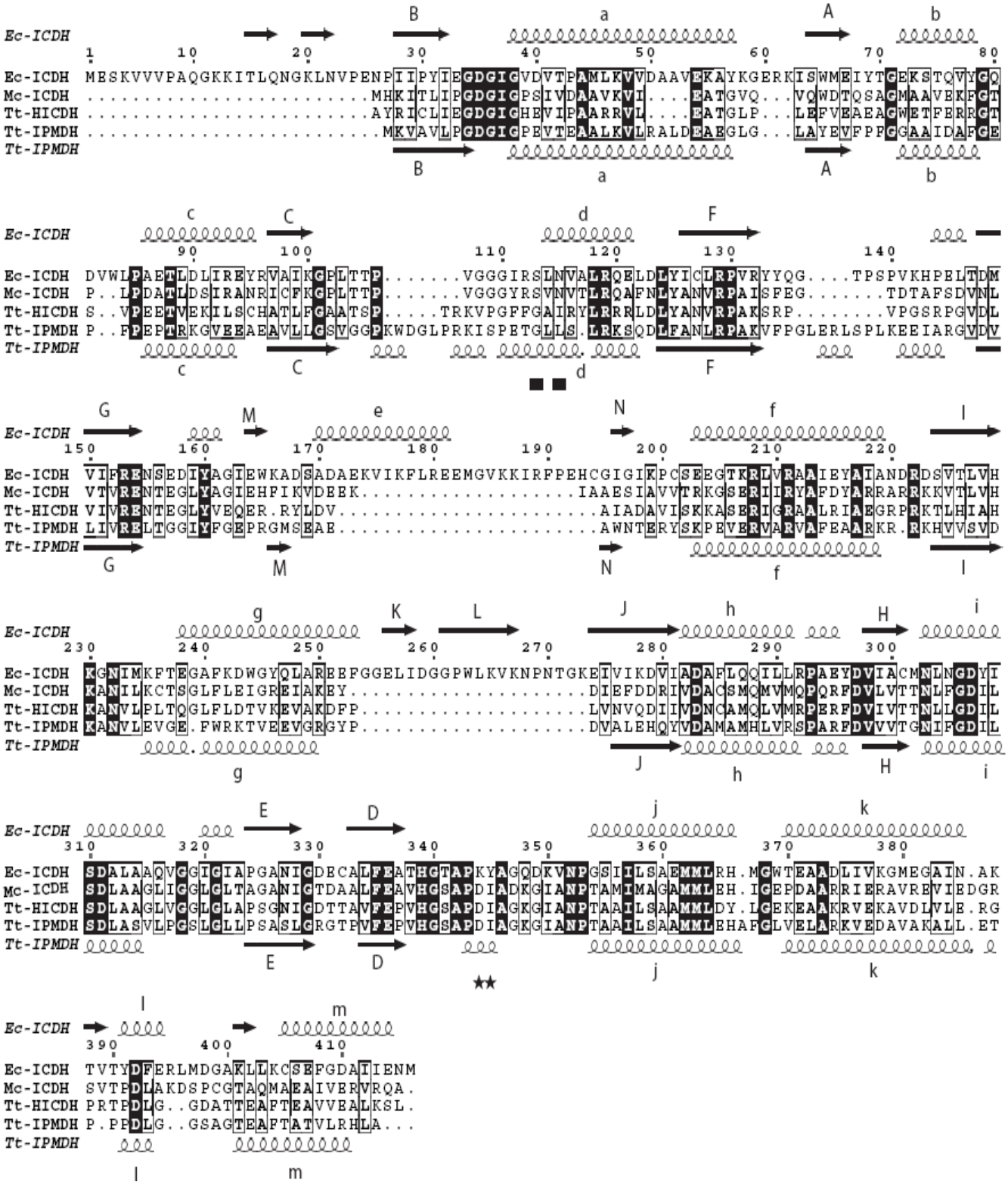

Fig.2

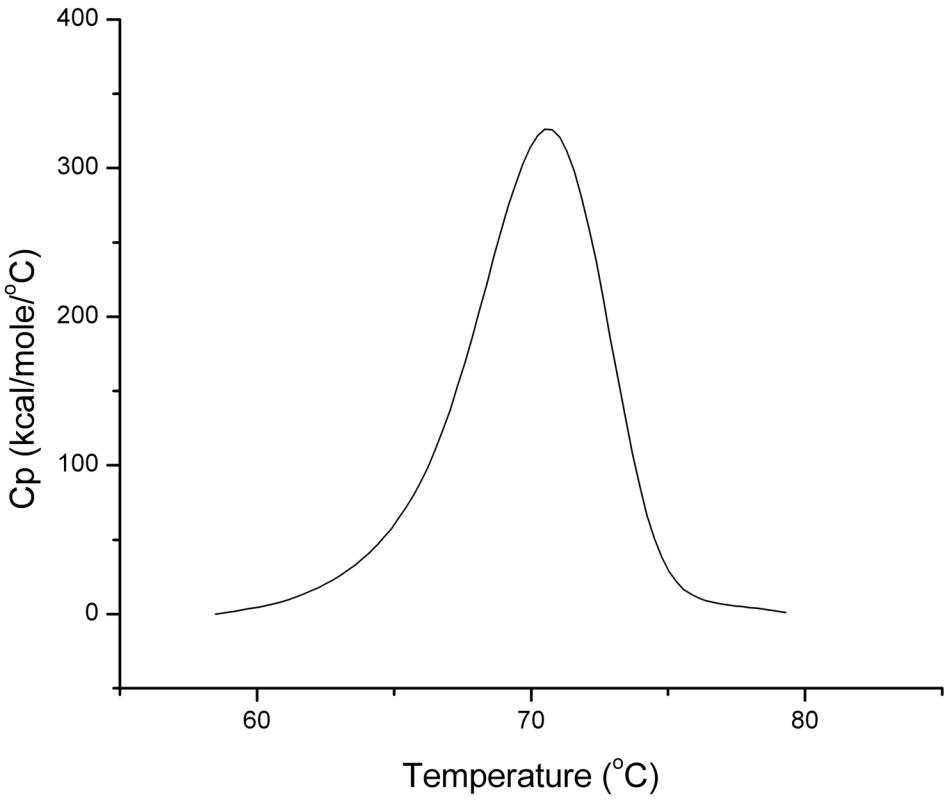

Fig.3

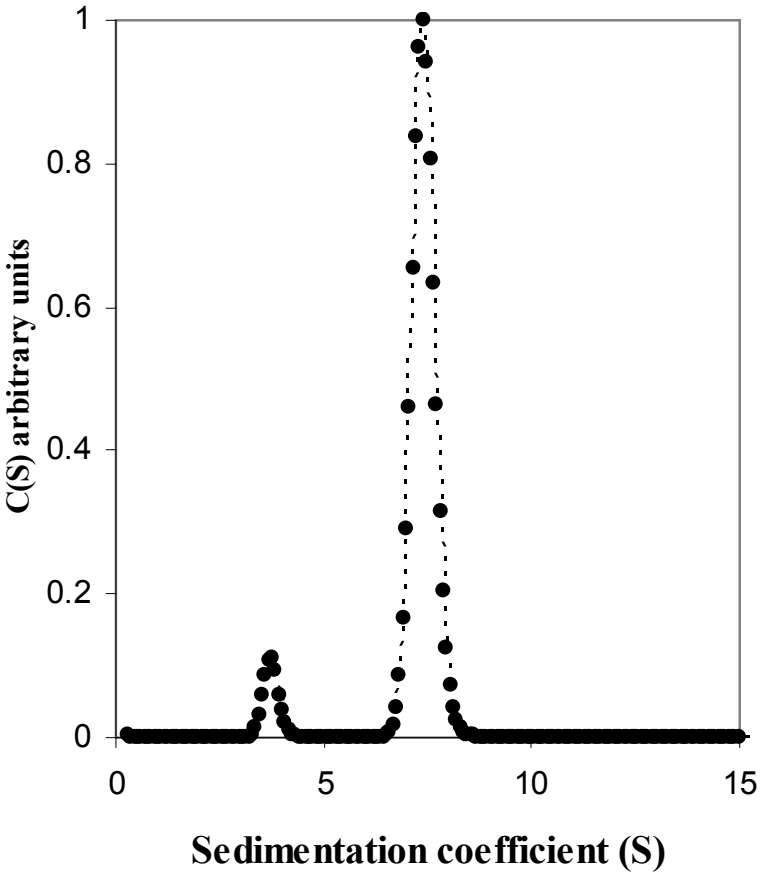
1
0.8
0.6
0.4
0.2
0
C(S) arbitrary units
0
5
10
15
Sedimentation coefficient (S)

Fig.4

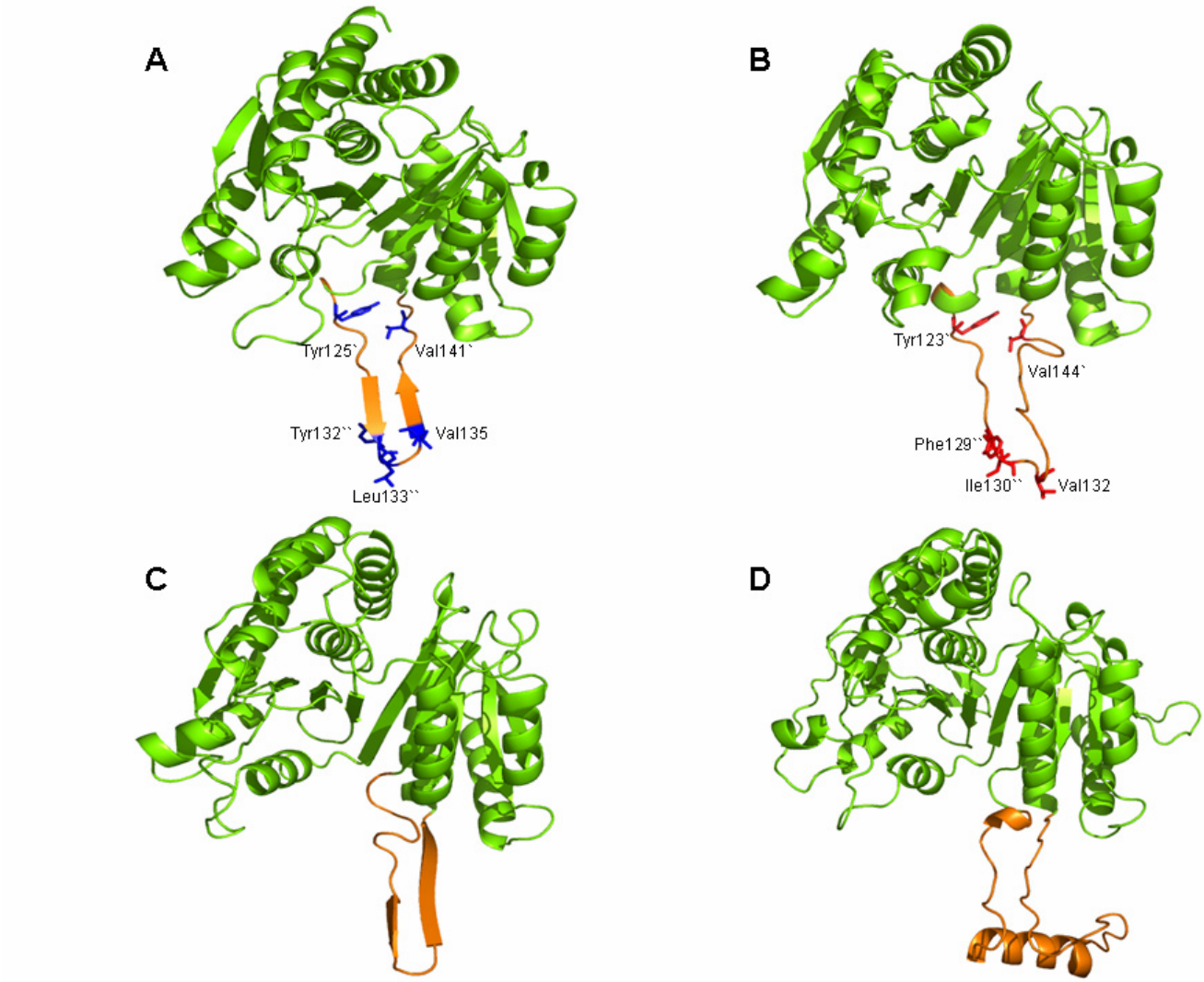
A
Tyr125`
Val141`
Tyr132``
Val135
Leu133``
B
Tyr123`
Val144`
Phe129``
Ile130``
Val132
C
D